Impact of the external resistance on the switching power consumption in VO_2 nano gap junctions

L. Sánchez, A. Rosa, A. Griol, A. Gutierrez, P. Homm, B. Van Bilzen, M. Menghini, J. P. Locquet, and P. Sanchis

Citation: Appl. Phys. Lett. **111**, 031904 (2017);
View online: https://doi.org/10.1063/1.4994326
View Table of Contents: http://aip.scitation.org/toc/apl/111/3
Published by the American Institute of Physics

Impact of the external resistance on the switching power consumption in VO_2 nano gap junctions

L. Sánchez,[1] A. Rosa,[1] A. Griol,[1] A. Gutierrez,[1] P. Homm,[2] B. Van Bilzen,[2] M. Menghini,[2] J. P. Locquet,[2] and P. Sanchis[1]
[1]*Nanophotonics Technology Center, Universitat Politècnica de València, Camino de Vera s/n, Valencia 46022, Spain*
[2]*Department of Physics and Astronomy, KU Leuven, Celestijnenlaan 200D, 3001 Leuven, Belgium*

(Received 11 April 2017; accepted 5 July 2017; published online 18 July 2017)

The influence of an external resistance on the performance of VO_2 nanogap junctions is analyzed and experimentally characterized. The current-voltage response shows the reversible metal-insulator transition typical of VO_2 based devices. When reaching the metallic state, the current through the VO_2 junction is abruptly increased, which may result in electrical contact damage. Therefore, an external resistance in series with the VO_2 junction is usually employed to limit the maximum current through the device. Our results indicate that the external resistance plays a key role in the switching power consumption showing an optimum value, which depends on the dimensions of the VO_2 junction. In such a way, power consumption reductions up to 90% have been demonstrated by selecting the optimum external resistance value. *Published by AIP Publishing.*
[http://dx.doi.org/10.1063/1.4994326]

Vanadium dioxide (VO_2) is a transition metal oxide specially considered for the integration with silicon photonics due to its reversible metal-insulator transition (MIT).[1] The switching between those states provides a change in the optical properties of the material useful for the development of ultra-compact optical devices based on the hybrid VO_2/Si technology.[2–7] The phase transition can be reached by means of the application of external stimuli like temperature,[8–10] electric field,[11–17] or optical pumping.[18,19] Together with the electronic phase transition, the material also shows a structural change from a monoclinic phase to a rutile phase[20] that is reached at a relatively low temperature in comparison with other phase change materials or other VO_x phases such as vanadium pentoxide.[21] Nevertheless, the origin of the phase transition has been the subject of intense discussion. Several works have studied the MIT in VO_2 to elucidate if its mechanism, when driven with an electric field, is mainly due to the electric-field contribution[16,22–24] or due to a Joule-heating process.[9,25,26]

To study the MIT using the electrical excitation, the most used structure is a nanojunction based on metal pads deposited over a VO_2 film with a defined gap between them.[11,14,16,17,22,24,26–28] By applying an electric field between the contacts, current flows through the VO_2 junction. The current-voltage response of the junction allows the electrical characterization of the MIT. When the metallic state is reached, the current through the VO_2 junction is abruptly increased due to a reduction in the VO_2 resistance. Such a current step may damage the contacts or even the VO_2 film. Thus, an external resistance connected in series with the VO_2 junction is required to limit the current after the MIT. In this letter, we show that the external resistance plays a key role not only to protect the device but also in the electrical power required to switch to the metallic state. Depending on the dimensions of the VO_2 junction, there is an optimum external resistance that results in a minimum power consumption.

Nanogap junctions were fabricated on VO_2 films with a thickness of 40 nm deposited on silicon substrates. Figure 1(a) shows the concept art of a nanogap junction and Fig. 1(b) shows SEM images of the fabricated structures with a gap of 0.5 μm and widths of 5 μm and 20 μm. Prior to electrode deposition, the VO_2 thin films were prepared following a similar two-step process to the one used on silicon substrates reported in Ref. 29. For the films used in the present work, an amorphous vanadium oxide (VO_x) film was first deposited by oxygen-assisted molecular beam epitaxy at room temperature and then transformed into polycrystalline VO_2 by *ex-situ* annealing at moderate temperatures. Details about the VO_2 growth process will be reported elsewhere. For the metal pad deposition, a polymer resist was spin-coated on the VO_2 film to pattern the electrodes by direct electron beam lithography. After developing the sample resist, 100 nm of Cu were deposited by electron-beam evaporation. Finally, a lift-off process was carried out by using a wet resist stripping procedure.

The characterization of the VO_2 junctions was carried out by using a Keithley 2440 5A SourceMeter. Figure 1(c) shows the voltage-current response and corresponding evolution of the VO_2 resistance for a junction with a width of 20 μm and an external resistance of 2 kΩ. Before the transition to the low resistance state, the relationship between the current and the applied voltage has been explained as a consequence of the Poole-Frenkel effect.[15,17] An electric field-assisted mechanism of carrier injection involving Joule heating induces the formation of a highly conductive filament between the metal pads, which originates the phase transition in the VO_2. The corresponding abrupt change in the VO_2 resistance is also clearly seen in Fig. 1(c). After reaching the threshold voltage ($V_{I\rightarrow M}$), the VO_2 switches from a high resistance state (insulating) to a low resistance state (metallic). In fact, after the transition, the slope of the current-voltage response is approximately given by the

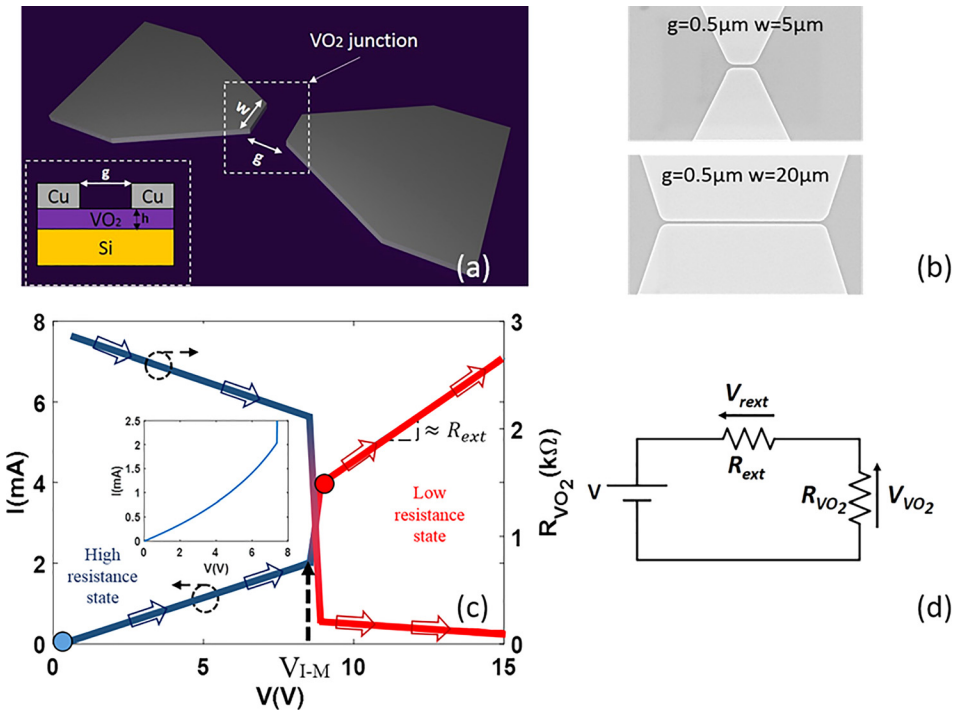

FIG. 1. (a) Schematic of the VO_2 junction. (b) SEM images of the fabricated structures. (c) Current–voltage response and corresponding VO_2 resistance (R_{VO2}) for a junction with a width of 20 μm and an external resistance of 2 kΩ. The current-voltage response before the transition (zoomed in the inset) shows an exponential behavior consistent with Poole-Frenkel conduction mechanism.[15,17] (d) Simplified schematic of the VO_2 electrical circuit.

external resistance demonstrating the abrupt resistance drop in the VO_2 patch. Considering the gap and the applied voltage at the source, the critical electric field ($E_c \approx V_{VO2}/g$) at the transition is around 10 V/μm, which is in agreement with the values reported in the literature.[26] The reverse transition from the metallic state to the insulating state is dominated by the thermal dissipation rates at the junction. In fact, the temperature reached by the VO_2 due to Joule heating, when the conductive filament is formed, limits the switching speed.

Figure 1(d) shows the simplified electrical schematic of the VO_2 junction. The resistances of the probes and the metal pads have been neglected and the parasitic capacitance parallel to the VO_2 resistance behaves as an open circuit in the DC regime. Therefore, the total resistance of the device consists of the resistance of the VO_2 junction plus the external resistance. When the applied voltage is high enough to induce the phase transition, the VO_2 reaches the metallic state and its resistance becomes very low. In this case, the total resistance may be reduced to the external resistance so that the electrical power required for switching to the metallic state can be expressed as

$$P \approx \frac{V_{I-M}^2}{R_{ext}}, \tag{1}$$

where $V_{I\to M}$ is the switching voltage applied by the source and R_{ext} is the external resistance. Taking into account the electrical scheme shown in Fig. 1(d), the switching voltage is given by

$$V_{I\to M} = V_{VO2}\left(1 + \frac{R_{ext}}{R_{VO2}}\right), \tag{2}$$

where V_{VO2} and R_{VO2} are the voltage and resistance at the VO_2 junction just before the transition to the metallic state, respectively. The power consumption defined by Eq. (1) can be minimized by increasing the external resistance. However, according to Eq. (2), the switching voltage will also increase, thus increasing the power consumption. Thereby, there will be a trade-off between both parameters. The minimum power consumption can be derived by inserting Eq. (2) in Eq. (1) and making the partial derivative with respect to the external resistance equal to zero

$$\frac{\partial P}{\partial R_{ext}} = \frac{2(\mathrm{R_{ext}} + \mathrm{R_{VO2}})}{\mathrm{R_{ext}}} - \frac{(\mathrm{R_{ext}} + \mathrm{R_{VO2}})^2}{\mathrm{R_{ext}^2}} = 0, \tag{3}$$

which gives an optimum value of $R_{ext} = R_{VO2}$. Therefore, the power consumption will be minimized for an external resistance similar to the VO_2 resistance in the insulating state. The influence of the external resistance on the power consumption has been experimentally characterized in the VO_2 junctions by using several external resistances with values below and above the VO_2 resistance. Figure 2 shows the applied switching voltage and the voltage at the VO_2 junctions as a function of the external resistance for widths of (a) 20 μm and (b) 5 μm, respectively. To induce the transition to the metallic state, the voltage applied to the VO_2 junction has to be enough to reach the critical electric field, and thereby, a low dependency with the external resistance is observed. The average voltages are around 4.75 V and 3.6 V for the junction widths of 20 μm and 5 μm, respectively. A smaller voltage is required for the narrower width despite both junctions have the same gap, thus indicating that this parameter has also some influence. On the other hand, the switching voltage applied at the source clearly increases when the external resistance is higher. This is in agreement with Eq. (2) because a higher voltage is needed to maintain the critical electric field at the VO_2 junction. Figure 2(c) and (d) show the current before and after the transition to the metallic state for the two different junction widths respectively. The voltage at the VO_2 junction and its resistance, which also shows a low dependency with the external resistance, determine the current before the

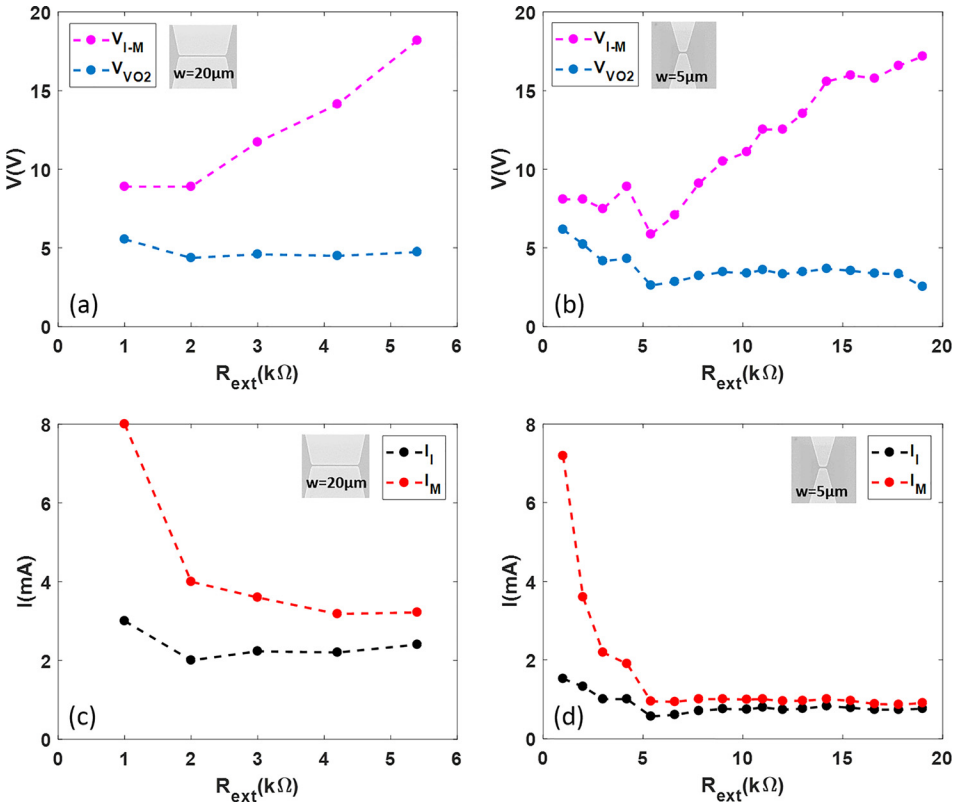

FIG. 2. Experimental results of (a) and (b) switching voltage at the source ($V_{I\rightarrow M}$) and corresponding voltage at the VO_2 gap (V_{VO2}) as a function of the external resistance and (c) and (d) electrical current before (I_I) and after (I_M) the transition to the metallic state for the VO_2 junctions shown in the insets.

transition. The VO_2 resistance is higher in the junction with a smaller width, and therefore, the current is lower. On the other hand, the current after the transition is limited when the external resistance is increased. In fact, the current tends to a value close to the one before the transition because the external resistance limits the current step across the VO_2 phase transition.

The variation of the VO_2 resistance as a function of the applied power for different values of external resistance is shown in Figs. 3(a) and 3(b). The VO_2 resistance at the phase transition changes from around 2.1 kΩ to 200 Ω for the width of 20 μm [see Fig. 3(a)] and from around 4.6 kΩ to 1 kΩ for the width of 5 μm [see Fig. 3(b)], showing an almost negligible influence of the external resistance. By comparing both

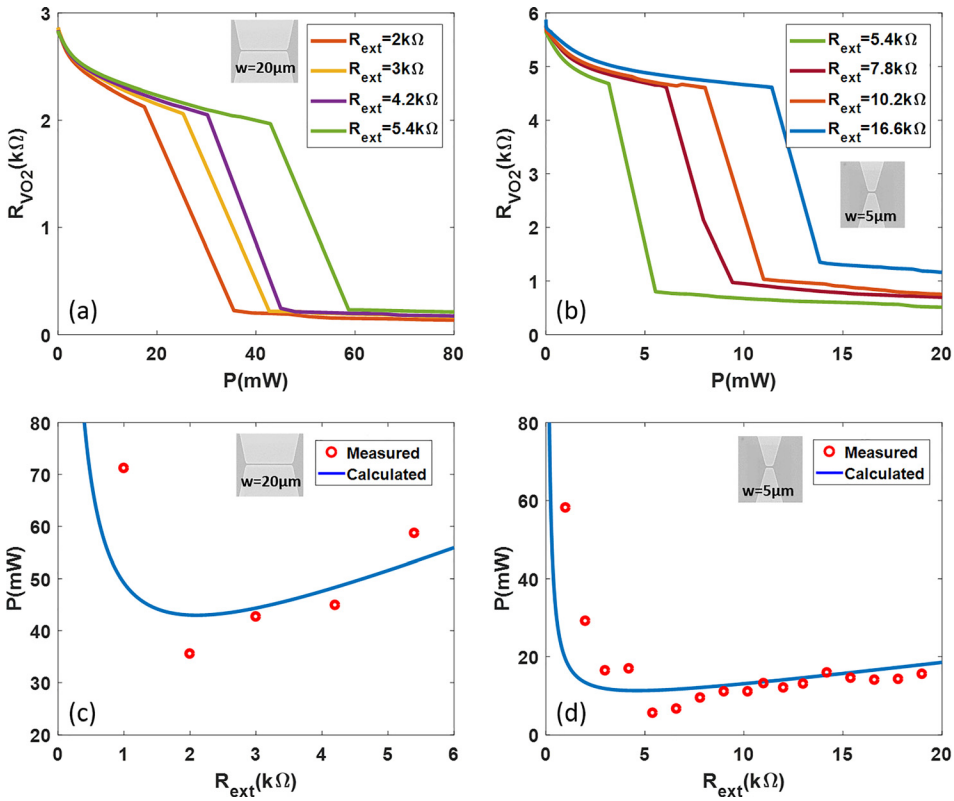

FIG. 3. (a), (b) Measured resistance of the VO_2 gap (R_{VO2}) as a function of the applied electrical power for different values of the external resistance. (c), (d) Measured and calculated (see text) power consumption as a function of the external resistance.

cases, the ratio between VO_2 resistances after the transition scales quite well with the change in the junction width and is more than two times higher than the ratio just before the transition. Such results indicate that the whole VO_2 section between the electrodes is converted into the metallic state after the transition while a non-uniform current flows across the VO_2 before the transition. The power consumption required to switch to the metallic state has been finally obtained. Figure 3(c) depicts the comparison between the calculated (blue line) and measured (red dots) results for the VO_2 junction with a width of 20 μm. The continuous curve has been obtained by using Eq. (1) where the switching voltage applied by the source has been replaced by Eq. (2) with $V_{VO2} = 4.75$ V extracted from Fig. 2(a) and $R_{VO2} = 2.1$ kΩ extracted from Fig. 3(a). Measurements are in good agreement with calculations showing the same tendency and a minimum power consumption of 35 mW for an external resistance of 2 kΩ. The same procedure has been followed to analyze the power consumption of the VO_2 junction with a width of 5 μm, shown in Fig. 3(d). In this case, the calculated power consumption has been obtained by using $V_{VO2} = 3.6$ V and $R_{VO2} = 4.6$ kΩ extracted from Figs. 2(b) and 3(b), respectively. Measurements are also in good agreement with calculations showing a minimum power consumption of 5.5 mW for an external resistance of 5.4 kΩ. Therefore, in both VO_2 junctions, the minimum power consumption for switching to the metallic state is achieved when the external resistance is similar to the resistance of the VO_2 gap, confirming the theoretical result obtained from Eq. (3).

In conclusion, we have demonstrated the influence of the external resistance on the power consumption of switching devices based on VO_2 junctions. The power consumption is minimized when the external resistance has a similar value to the resistance of the VO_2 patch in the insulating state. To match both resistances, several parameters like the dimensions of the VO_2 patch can be properly designed. A power consumption reduction between 50% and 90% has been demonstrated with the selection of the optimum external resistance. These results are relevant for developing efficient electro-optical switching devices based on the VO_2 phase transition. Furthermore, they could be also of interest for the development of low power non-volatile resistive memories.[30]

This work was supported by the European Commission under Project No. FP7-ICT-2013-11-619456 SITOGA. Financial support from TEC2016-76849-C2-2-R and NANOMET Conselleria de Educació, Cultura i Esport-PROMETEOII/2014 034 is also acknowledged. P.H. acknowledges support from Becas Chile-CONICYT.

[1]G. Seo, B. J. Kim, C. Ko, Y. Cui, Y. W. Lee, J. H. Shin, S. Ramanathan, and H. T. Kim, IEEE Electron Device Lett. **32**, 1582 (2011).
[2]R. M. Briggs, I. M. Pryce, and H. A. Atwater, Opt. Express **18**, 11192 (2010).
[3]L. Sanchez, S. Lechago, and P. Sanchis, Opt. Lett. **40**, 1452 (2015).
[4]A. Joushaghani, J. Jeong, S. Paradis, D. Alain, J. S. Aitchison, and J. K. S. Poon, Opt. Express **23**, 3657 (2015).
[5]L. Sánchez, F. C. Juan, A. Rosa, and P. Sanchis, J. Opt. **19**, 035401 (2017).
[6]M. A. Kats, R. Blanchard, P. Genevet, Z. Yang, M. M. Qazilbash, D. N. Basov, S. Ramanathan, and F. Capasso, Opt. Lett. **38**, 368 (2013).
[7]L. Sanchez, S. Lechago, A. Gutierrez, and P. Sanchis, IEEE Photonics J. **8**, 1 (2016).
[8]C. Ko and S. Ramanathan, Appl. Phys. Lett. **93**, 252101 (2008).
[9]A. Zimmers, L. Aigouy, M. Mortier, A. Sharoni, S. Wang, K. West, J. Ramirez, and I. Schuller, Phys. Rev. Lett. **110**, 056601 (2013).
[10]M. M. Qazilbash, M. Brehmmm, B.-G. Chae, P.-C. Ho, G. O. Andreev, B.-J. Kim, S. J. Yun, A. V. Balatsky, M. B. Maple, F. Keilmann, H.-T. Kim, and D. N. Basov, Science **318**, 1750 (2007).
[11]B. G. Chae, H. T. Kim, D. H. Youn, and K. Y. Kang, Physica B **369**, 76 (2005).
[12]D. Ruzmetov, G. Gopalakrishnan, J. Deng, V. Narayanamurti, and S. Ramanathan, J. Appl. Phys. **106**, 083702 (2009).
[13]S. B. Lee, K. Kim, J. S. Oh, B. Kahng, and J. S. Lee, Appl. Phys. Lett. **102**, 063501 (2013).
[14]A. Joushaghani, J. Jeong, S. Paradis, D. Alain, J. Stewart Aitchison, and J. K. S. Poon, Appl. Phys. Lett. **104**, 221904 (2014).
[15]P. Markov, R. E. Marvel, H. J. Conley, K. J. Miller, R. F. Haglund, and S. M. Weiss, ACS Photonics **2**, 1175 (2015).
[16]Z. Yang, S. Hart, C. Ko, A. Yacoby, and S. Ramanathan, J. Appl. Phys. **110**, 033725 (2011).
[17]J. Yoon, G. Lee, C. Park, B. S. Mun, and H. Ju, Appl. Phys. Lett. **105**, 083503 (2014).
[18]J. D. Ryckman, V. Diez-Blanco, J. Nag, R. E. Marvel, B. K. Choi, R. F. Haglund, Jr., and S. M. Weiss, Opt. Express **20**, 13215 (2012).
[19]J. D. Ryckman, K. A. Hallman, R. E. Marvel, R. F. Haglund, and S. M. Weiss, Opt. Express **21**, 10753 (2013).
[20]J. G. Ramírez, R. Schmidt, A. Sharoni, M. E. Gómez, I. K. Schuller, and E. J. Patiño, Appl. Phys. Lett. **102**, 063110 (2013).
[21]E. E. Chain, Appl. Opt. **30**, 2782 (1991).
[22]E. Freeman, G. Stone, N. Shukla, H. Paik, J. A. Moyer, Z. Cai, H. Wen, R. Engel-Herbert, D. G. Schlom, V. Gopalan, and S. Datta, Appl. Phys. Lett. **103**, 263109 (2013).
[23]G. Gopalakrishnan, D. Ruzmetov, and S. Ramanathan, J. Mater. Sci. **44**, 5345 (2009).
[24]J. Leroy, A. Crunteanu, A. Bessaudou, F. Cosset, C. Champeaux, and J. C. Orlianges, Appl. Phys. Lett. **100**, 213507 (2012).
[25]S. Kumar, M. D. Pickett, J. P. Strachan, G. Gibson, Y. Nishi, and R. S. Williams, Adv. Mater. **25**, 6128 (2013).
[26]B. S. Mun, J. Yoon, K. S. Mo, K. Chen, N. Tamura, C. Dejoie, M. Kunz, Z. Liu, C. Park, K. Moon, and H. Ju, Appl. Phys. Lett. **103**, 061902 (2013).
[27]J. B. Kim, Y. W. Lee, B. G. Chae, S. J. Yun, S. Y. Oh, H. T. Kim, and Y. S. Lim, Appl. Phys. Lett. **90**, 023515 (2007).
[28]I. P. Radu, B. Govoreanu, S. Mertens, X. Shi, M. Cantoro, M. Schaekers, M. Jurczak, S. De Gendt, A. Stesmans, and M. Heyns, Nanotechnology **26**, 165202 (2015).
[29]B. Van Bilzen, P. Homm, L. Dillemans, C. Y. Su, M. Menghini, M. Sousa, C. Marchiori, L. Zhang, J. W. Seo, and J. P. Locquet, Thin Solid Films **591**, 143 (2015).
[30]M. Saremi, Micro Nano Lett. **11**, 762 (2016).